Environmental Controls on Diffusive and Ebullitive Methane Emission at a Sub-Daily Time Scale in the Littoral Zone of a Mid-Latitude Shallow Lake

T. Taoka[1], H. Iwata[1], R. Hirata[2], Y. Takahashi[2], Y. Miyabara[3], and M. Itoh[4]

[1]Department of Environmental Science, Faculty of Science, Shinshu University, Matsumoto, Japan.

[2]Center for Global Environmental Research, National Institute for Environmental Studies, Tsukuba, Japan.

[3]Education and Research Center for Inland Water and Highland Environments, Faculty of Science, Shinshu University, Matsumoto, Japan.

[4]School of Human Science and Environment, University of Hyogo, Himeji, Japan.

Corresponding author: Hiroki Iwata (hiwata@shinshu-u.ac.jp)

Key Points:

- Diffusive and ebullitive methane fluxes from a shallow lake were examined for their environmental controls at a sub-daily time scale.
- Diffusive flux was controlled by wind speed and transfer of accumulated dissolved methane from the bottom layer to the surface layer.
- In addition to triggers related to wind and pressure, the accumulation of bubbles in the sediment is an important factor for ebullition.

Abstract

Environmental controls on methane (CH_4) emission from lakes are poorly understood at sub-daily time scales due to a lack of continuous data, especially for ebullition. We used a novel technique to partition eddy covariance CH_4 flux observed in the littoral zone of a mid-latitude shallow lake in Japan and examined the environmental controls on diffusion and ebullitive CH_4 flux separately at a sub-daily time scale during different seasons. Both diffusive and ebullitive flux were significantly higher in summer than winter. The contribution of ebullitive flux to total flux was 56% on average. Diffusive flux increased with increasing wind speed due to increased subsurface turbulence. For a given wind speed, diffusive flux was higher in summer than in winter due to the higher concentration of dissolved CH_4 in the surface water during summer. The transfer of accumulated dissolved CH_4 from the bottom layer to the surface in summer and the accumulation of dissolved CH_4 under surface ice in winter were important for explaining the variability of diffusive flux. In summer, ebullition tended to occur following triggers such as a decrease in hydrostatic pressure or an increase in wind speed. In winter, on the other hand, the impact of triggers was not obvious, and ebullition tended to occur in the morning when the wind speed began to increase. The low CH_4 production rate in winter slowed the replenishment of bubbles in the sediment, negating the effect of triggers on ebullition.

Plain Language Summary

Lakes are one of the main natural sources of methane (CH_4). Methane is emitted from lake sediments to the atmosphere via diffusion through the water column and episodic emission of bubbles (ebullition). To improve prediction of CH_4 emission from lakes, it is necessary to clarify the environmental controls on CH_4 emission processes. However, environmental controls at sub-daily time scales are poorly understood due to a lack of continuous data, especially for ebullition. We applied a novel technique to partition continuous CH_4 flux data obtained with the eddy covariance technique in a mid-latitude shallow lake into diffusive and ebullitive fluxes, and examined their environmental controls separately. The diffusive flux increased with increasing wind speed and increasing dissolved CH_4 concentrations in the surface water. For this shallow lake, the transfer of accumulated dissolved CH_4 from the bottom layer to the surface under thermally stratified conditions was important for explaining the variability of diffusive flux. In summer, ebullition tended to occur following triggers such as a decrease in hydrostatic pressure or an increase in wind speed. In winter, on the other hand, the low CH_4 production rate slowed the replenishment of bubbles in the sediment, negating the effect of triggers on ebullition.

1 Introduction

Lakes are one of the main natural sources of methane (CH_4), which is an important greenhouse gas (e.g., Forster et al., 2007). Using bottom-up approaches, a recent global synthesis estimated CH_4 emissions from fresh waters as 60-180 Tg CH_4 $year^{-1}$ (Saunois et al., 2016). However, considerable uncertainty remains, partly stemming from the large spatiotemporal variability of CH_4 emissions from lakes. Therefore, elucidating the variation and underlying mechanisms of emissions is necessary to address this uncertainty.

CH_4 is mainly produced in anoxic lake sediments by methanogenic bacteria and is emitted to the atmosphere via three emission pathways: diffusion within the water column,

diffusion within plant aerenchyma, and ebullition (bubble emission). These emissions are controlled by different physical and biological constraints (e.g., Bastviken et al., 2004).

Diffusive emission at the air–water interface is strongly affected by wind speed because increased wind speed results in enhanced subsurface turbulence through formation of velocity shear in surface waters and waves (Cole and Caraco, 1998; Bock et al., 1999), which increases the emission efficiency. In addition to wind speed, thermal instability within the water column due to surface cooling increases subsurface turbulence (MacIntyre et al., 2010; Tedford et al, 2014; Heiskanen et al., 2014). Diffusion also depends on the concentration difference between the water surface skin layer and the bulk surface water below (Wanninkhof et al., 2009). The concentration of dissolved CH_4 in the surface water is controlled by seasonal variation in CH_4 production in the sediments (Thebrath et al., 1993; Liikanen et al., 2003) and CH_4 oxidation within the water column (Utsumi et al., 1998; Schubert et al., 2012), as well as by water mixing. Water mixing is affected by wind and thermal instability of the water. During stably stratified periods following surface ice formation, CH_4 produced in the sediments is trapped below the thermocline. Subsequently, during periods of whole-lake mixing after ice melt, the accumulated dissolved CH_4 is transported to the lake surface, enhancing emission to the atmosphere (Jammet et al., 2015; Podgrajsek et al., 2016; Jansen et al., 2019).

Ebullition is thought to occur (1) when the sediment is disturbed by physical stress, assuming that bubbles have accumulated in the sediment, or (2) when bubbles reach a sufficiently large size to become buoyant. Momentum transfer to the lake sediment layer, driven by wind or an internal seiche introduces physical stress to the sediment, which can force bubbles to be released (Joyce and Jewell, 2003). Bubbles can grow through physical expansion due to hydrostatic pressure and temperature changes and addition of gases when decreasing hydrostatic pressure and/or warming sediments reduced gas solubility (e.g., Fechner-Levy and Hemond, 1996; Tokida et al., 2007; Wik et al., 2013).

CH_4 emission from lakes and its environmental controls have been traditionally examined using floating chambers or bubble traps. Due to the small spatial coverage and limited time resolution of these methods, however, it is difficult to obtain spatiotemporally representative flux data and to clarify environmental controls in details, especially for highly variable ebullition. Emissions are often controlled in a nonlinear fashion, suggesting that data with high temporal resolution are necessary to elucidate detailed control mechanisms. Conversely, the eddy covariance technique enables us to obtain data of continuous flux originating from a larger footprint, rendering it useful for quantifying temporally and spatially variable CH_4 emissions from a lake, including diffusive and ebullitive emissions.

Sub-daily variation in CH_4 flux from lakes and reservoirs has been reported in previous eddy covariance studies (Eugster et al., 2011; Podgrajsek et al., 2014; Deshmukh et al., 2014; Jammet et al., 2017; Rey-Sanchez et al., 2018). Studies in boreal lakes have reported diurnal variations with a peak early in the morning (Podgrajsek et al., 2014; Jammet et al., 2017), whereas studies in hydropower reservoirs observed a maximum when the artificially controlled water level was lowest. Deshmukh et al. (2014) reported a clear diurnal bimodal pattern, with the first peak occurring around noon and the second at midnight, whereas Eugster et al. (2011) reported a maximum in the evening. These authors speculated that the maximum emissions reflected an increase in ebullition.

One limitation of the eddy covariance technique is that it cannot distinguish emission pathways, which was responsible, in part, for the ambiguous interpretation of environmental controls on flux in previous studies. Recently, we developed a technique to partition eddy covariance CH_4 flux into diffusive and ebullitive fluxes (Iwata et al., 2018); this technique has the potential to elucidate environmental controls of diffusive and ebullitive CH_4 emissions at sub-daily time scales. In addition, in most lake models (Subin et al., 2012; Stepanenko et al., 2016), these emission pathways are explicitly represented at sub-daily time scales; thus, the partitioned flux data are useful to parameterize and validate these lake models.

In this study, we applied this partitioning technique to CH_4 flux measured with the eddy covariance technique for a whole year in the littoral zone of a mid-latitude shallow eutrophic lake in Japan. The objectives were to quantify the contributions of diffusive and ebullitive flux in the littoral zone, examine the controlling mechanisms of diffusive and ebullitive fluxes separately at a sub-daily time scale, and determine whether the controls vary by seasons.

2 Observation and Data Analysis

2.1 Study site

Measurements were conducted at the southeast shore of Lake Suwa (Fig. 1), a shallow eutrophic lake located at 759 m a.s.l. in the center of Nagano Prefecture, Japan (Park et al., 1998; Ikenaka et al., 2005). The total area of the lake is 13.3 km^2, and the mean and maximum depths are approximately 4 m and 6.9 m, respectively. The water level is artificially controlled by a water gate and is generally 0.2 m higher in winter than in summer. Around the observation site, water caltrop (*Trapa japonica* Flerow, a floating-leaved plant) and Esthwaite waterweed (*Hydrilla verticillata* [L.f.] Royle, a submerged plant) can be seen near the lake shore during summer. A notable feature of this lake is that there are areas of continuous bubble emission, one of which is located 55 m from the observation mast at a direction of 325° (Fig. 1b, Iwata et al., 2018).

The lake is surrounded by cities with a combined population of more than 180,000 inhabitants; thus, the lake receives considerable anthropogenic inputs. Dense algal blooms are regularly observed during the summer (Park et al., 1998).

The annual mean air temperature (1988–2017) in this area is 11.3℃; the January and August monthly means are −1.0℃ and 23.9℃, respectively. The mean annual precipitation is 1,310 mm. Figure S1 shows the distribution of wind directions during winter (from December 2017 to February 2018) and summer (from June to August 2018). The prevailing wind was northwesterly for the lake side from the observation mast.

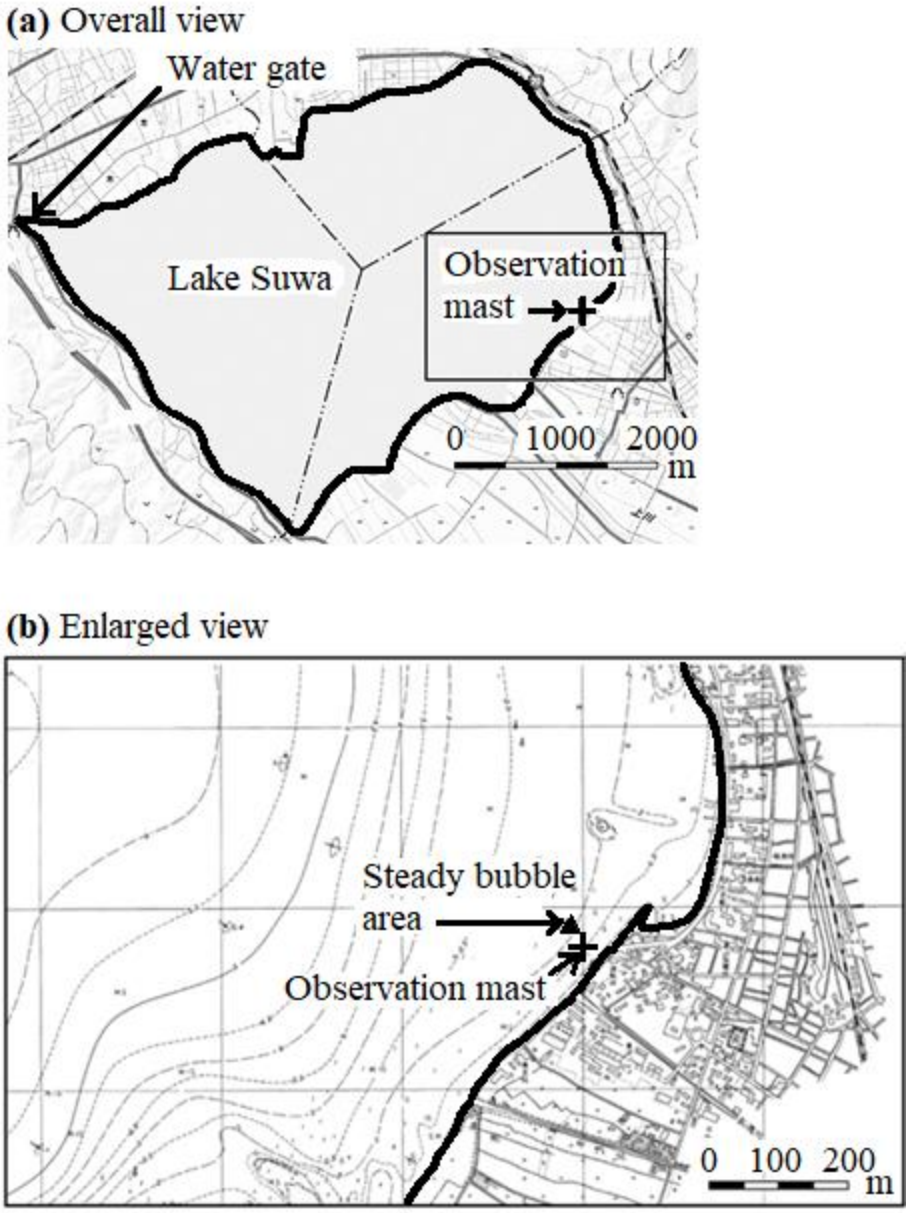

Figure 1. The **(a)** overall and **(b)** enlarged view of Lake Suwa. The plus in both maps represents the location of the observation mast. The triangle in **(b)** represents an area with steady bubble emission (Iwata et al., 2018). The figure is produced based on a map published by the Geospatial Information Authority of Japan.

2.2 Observations

Measurements were conducted from a pier (36°2′47.66″N, 138°6′30.07″E) on the southeast shore of the lake, where the water depth was approximately 2 m. The installed eddy-covariance system consisted of an ultrasonic anemo-thermometer (CSAT3; Campbell Scientific, Logan, UT, USA), open-path CH_4 analyzer (LI-7700; Li-Cor, Lincoln, NE, USA), open-path carbon dioxide (CO_2) / water vapor (H_2O) analyzer (EC-150; Campbell Scientific), and data logger (CR3000; Campbell Scientific). The observation height was about 3.2 m during summer,

though it changed depending on water level during the observation period. The horizontal distances of the sensors from the ultrasonic anemo-thermometer were 0.25 m for the CH_4 analyzer and 0.05 m for the CO_2/H_2O analyzer. Footprint analysis using a model from Kormann and Meixner (2001) indicated that the 90% flux footprint was typically 300–500 m from the observation mast, so the observed flux represents the emission from the littoral zone of this lake.

Along with eddy covariance measurements, we obtained meteorological and limnological data. Using the same data logger, we recorded 30-min means of wind speed (CSAT3), radiation balance (CNR4; Kipp and Zonen, Delft, The Netherlands), atmospheric pressure (PTB110; Vaisala, Helsinki, Finland), air temperature (HMP60; Vaisala), water and sediment temperature profiles (107; Campbell Scientific), and water level (CS451; Campbell Scientific). The water temperature was observed at five depths: 0.25, 0.5, 1.0, and 1.5 m below the water surface and 0.2 m above the local lake bottom. The top four sensors were attached to a wood pole with a float so that the measurement depth was constant regardless of water-level change. The sediment temperature was observed at depths of 0.05 and 0.2 m.

To measure dissolved CH_4 concentration, we manually sampled the water at seven depths (0, 0.1, 0.5, 1.0, 1.3, and 1.5 m below the water surface and 0.2 m above the local lake bottom) at approximately 1-month time intervals. Water samples at each depth were collected in three 30-mL glass vials using a silicon tube and a syringe, and dissolved CH_4 concentration was measured using the headspace technique (Itoh et al., 2015) with a gas chromatograph (GC-14B; Shimazu, Kyoto, Japan). Finally, we calculated dissolved CH_4 concentration at each depth using the ideal gas law and Bunsen solubility coefficient (Magen et al, 2014) and averaged the values from the three samples. The readers are referred to Iwata et al. (submitted) for more details. In this study, the surface (0 m) and bottom (0.2 m above the local lake bottom) data were used to explain the seasonal variation in diffusive flux.

2.3 Flux calculation and data analysis

The diffusive and ebullitive CH_4 fluxes were calculated for each 30-min period using the eddy covariance technique with flux partitioning (Iwata et al., 2018). Before the calculation, data spikes were removed (Vickers and Mahrt, 1997). Coordinate rotation of the observed wind vectors was performed so that the mean lateral and vertical wind velocities were equal to zero for each 30-min period. Data from the CH_4 and CO_2/H_2O analyzer were synchronized with those from sonic anemometer using cross-correlation analysis (Iwata et al., 2014). The 10 Hz data were then corrected point by point (Detto and Katul, 2007, Detto et al., 2011) for the effect of water vapor density on sonic virtual temperature (Schotanus et al., 1983) and for the air density variation (Webb et al., 1980) and spectroscopic effects (McDermitt et al., 2011) on CH_4 density. Then, a partitioning method developed in Iwata et al. (2018) was applied to calculate diffusive and ebullitive CH4 fluxes.

This partitioning method uses the scalar similarity concept between CH_4 molar density and other reference scalars in the wavelet time-scale domain. It assumes that turbulent fluctuation in CH_4 density, similar to a reference scalar with a spatially homogeneous source, is due to diffusive emission, and ebullitive emission locally violates that similarity. We selected H_2O density as the reference scalar, because the fluctuation of H_2O density is less affected by non-local atmospheric processes, such as entrainment and advection, than that of temperature at

this site (Iwata et al., 2018). To separate the diffusive and ebullitive components, wavelet coefficients for CH_4 density and H_2O density were compared in a scatter plot, and coefficients deviating from a regression line fitted to the coefficients were considered ebullitive components. For each month, we determined root mean squared deviations (RMSDs) around the regression line from visually selected 30-min 10 Hz data (n = 4) in which H_2O density and CH_4 density had global similarity. Assuming that the deviations from the regression line were normally distributed, we defined coefficients inside and outside ±3×RMSD bounds corresponding to diffusive and ebullitive flux, respectively.

The analysis was conducted for data obtained from September 2017 to August 2018. We used only flux data with wind blowing from 230–300° to eliminate data affected by the land surface and steady CH_4 bubble emission. The fluxes obtained from this sector showed low spatial variation with large episodic fluxes (Iwata et al. submitted), representing littoral CH_4 emission typical of similar lakes. General quality control (Vickers and Mahrt, 1997; Mahrt, 1998) was applied to assure flux data quality. Additionally, data affected by possible non-local processes were removed from the analysis because non-local processes can affect the scalar similarity, making the partitioning ambiguous. The effect of non-local processes was investigated in the flux–variance relationship (De Bruin et al., 1993; van de Boer et al., 2014) for H_2O density, where data deviating from the universal function with locally adjusted parameters were removed. Data with ebullitive flux <0 μmol m^{-2} s^{-1} or diffusive flux <-0.05 μmol m^{-2} s^{-1} (137 data points) were also eliminated. The data processing and selection criteria left 2,647 diffusive and ebullitive flux data points (15% of the whole) remaining for the analysis. In this manuscript, data from December 2017 to February 2018 represent winter, and data from June to August 2018 represent summer, unless otherwise specified.

3 Results and Discussion

3.1 Meteorological and limnological conditions

In summer, the daily average lake surface temperature was higher than the bottom temperature by 0.2–4.0℃ (Fig. 2b), indicating that the lake was stably stratified when net radiation was high (Fig. 2a). During winter, the lake surface and bottom temperatures were nearly identical, indicating that the lake was well mixed, except from late January to the middle of February. During that period, the lake surface was frozen, and the surface temperature was close to zero, whereas the bottom temperature was about 4℃, resulting in stable stratification. Hydrostatic pressure was, on average, higher in winter than in summer (Fig. 2c), mainly because the water level was artificially maintained at a greater depth in winter than in summer by a water gate. Additionally, week-scale fluctuations of hydrostatic pressure were observed, which were mainly caused by passage of low- and high-atmospheric-pressure systems. The wind speed tended to be higher in March–April on average, and sudden increases in daily mean wind speed coincided with the passage of strong low-pressure systems. The dissolved CH_4 concentration was higher in summer for both the surface and bottom layer (Fig. 2d). Dissolved CH_4 accumulated during summer, especially in the bottom layer, because of stable stratification. Data obtained after surface ice melt in February showed increased concentrations for both the surface and bottom layer. This accumulation was caused by the physical blockage of CH_4 diffusion to the atmosphere by the surface ice.

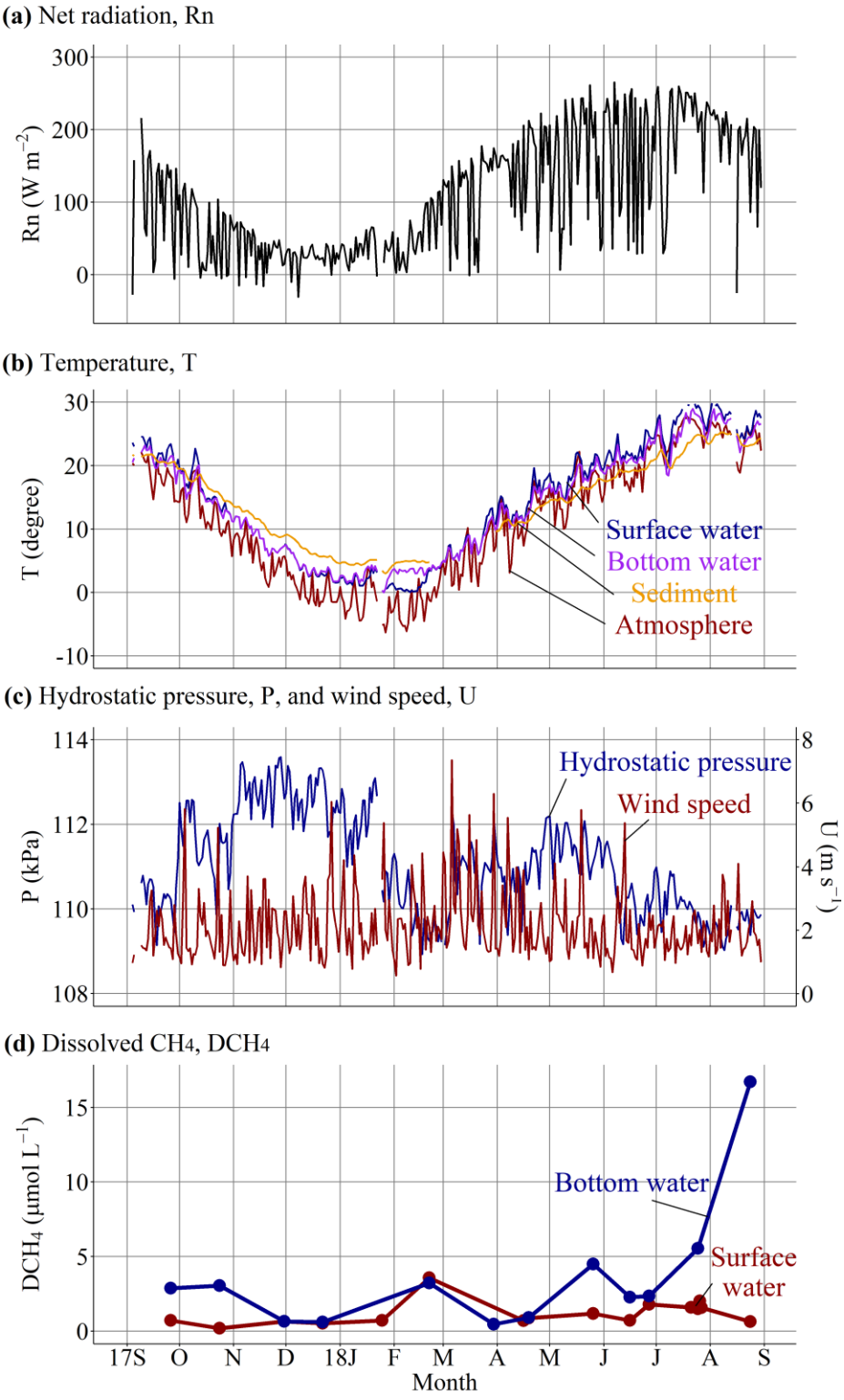

Figure 2. Seasonal variations in **(a)** net radiation; **(b)** temperatures of air (red), surface water (0.25 m depth: blue), bottom water (0.2 m above the local lake bottom: purple), and sediment (0.2 m depth: orange); **(c)** hydrostatic pressure (blue) and wind speed (red); and **(d)** dissolved

247 CH_4 concentration in the surface (0 m depth: red) and bottom (0.2 m above the local lake bottom:
248 blue) layer.

249

250 3.2 Seasonal variations in diffusive and ebullitive methane flux

251 Both diffusive and ebullitive CH_4 flux were significantly higher in summer than in winter
252 (Fig. 3). Mean diffusive CH_4 fluxes in winter and summer were 0.01 and 0.09 μmol m^{-2} s^{-1},
253 respectively, and mean ebullitive CH_4 fluxes in winter and summer were 0.02 and 0.12 μmol m^{-2}
254 s^{-1}, respectively. Incubation experiments using sediments from the same lake (Iwata et al.,
255 submitted) and other lakes (Duc et al., 2010) have shown that higher sediment temperatures in
256 summer can enhance CH_4 production in the sediment, thereby increasing diffusive and ebullitive
257 fluxes in summer.

258 Diffusive CH_4 flux had a relatively normal distribution: the skewness was −0.19 and 1.31
259 for winter (January 2018) and summer (July 2018), respectively (Fig. S2). The ebullitive CH_4
260 flux in winter had a positively skewed distribution (skewness, 7.14), whereas the distribution in
261 summer was relatively normal (1.21). The high positive skewness in winter indicates that the
262 larger ebullitive flux in winter occurred more episodically than that in summer.

263 Ebullitive CH_4 flux contributed 60% of the total flux in winter, 57% in summer, and 56%
264 annually, showing that both diffusion and ebullition are dominant pathways of CH_4 emission in
265 this shallow lake. Generally, ebullitive flux is thought to contribute 40–60% of total fluxes from
266 open water, and its contribution to total flux decreases with increasing lake size (Bastviken et al.,
267 2004). In a study conducted in three lakes and ten ponds in northern North America, ebullitive
268 CH_4 flux accounted for 18–23% of the total CH_4 fluxes for lakes, and ~56 % of total flux for
269 ponds (DelSontro et al., 2016). Conversely, in a meta-analysis (Bastviken et al., 2011), the
270 relative contributions of ebullition were much higher on average (70–90%) for lakes across all
271 latitude bands. The episodic nature of ebullition is probably responsible for the considerable
272 uncertainty in estimations of its relative contributions. It should be noted that the CH_4 flux
273 observed in our lake represents emission from the littoral zone, where ebullition is known to
274 occur more frequently than in the pelagic deep zone due to higher CH_4 production and lower
275 hydrostatic pressure (DelSontro et al., 2016; Itoh et al., 2017). Thus, the contribution of
276 ebullition may be lower when also accounting for CH_4 flux in the pelagic zone of this lake.

277 To roughly estimate the annual total emission from Lake Suwa, we assumed that the
278 mean diurnal variations in diffusive and ebullitive fluxes for each month obtained from the
279 selected data were representative of the flux for the whole month. Based on the mean diurnal
280 variations, mean daily fluxes for each month were calculated and multiplied by the amount of
281 time in the month to deduce the monthly total flux. Thus, by then summing over 12 months, we
282 obtained annual CH_4 fluxes of 17.6 and 19.3 g CH_4 m^{-2} $year^{-1}$ for diffusion and ebullition,
283 respectively, and a total flux of 36.9 g CH_4 m^{-2} $year^{-1}$.

284

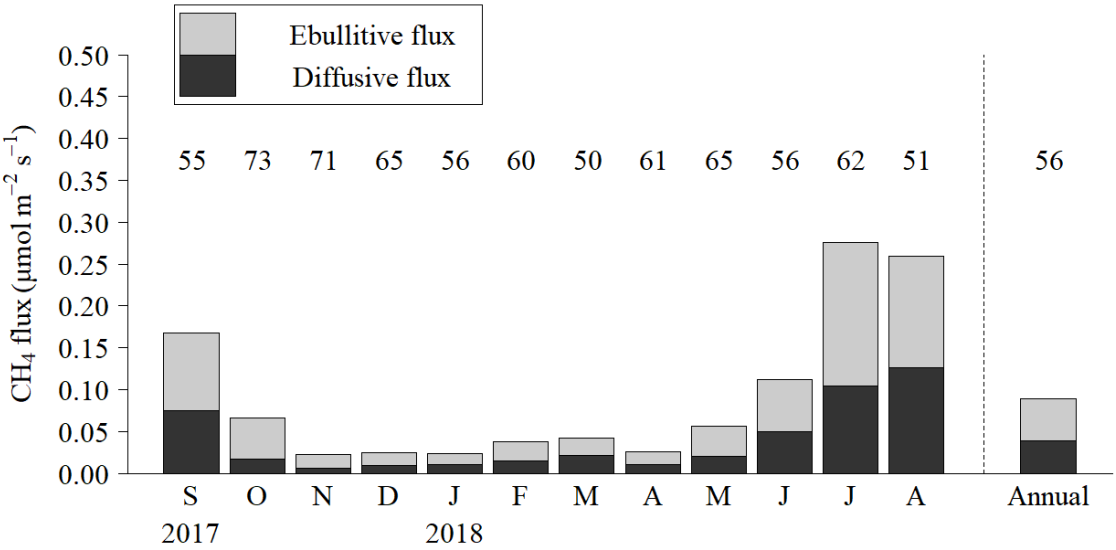

Figure 3. Seasonal variations in diffusive (black bar) and ebullitive (grey bar) CH_4 fluxes. The numbers above the bar indicate the contribution (%) of ebullitive flux to the total CH_4 flux (i.e., diffusive plus ebullitive flux). The rightmost bar shows the annual average calculated as the average of monthly averages.

3.3 Sub-daily variation in diffusive flux

At a sub-daily time scale, diffusive flux was high in the afternoon (Fig. 4c, d) in both summer and winter when wind speed increased (Fig. 4a, b). Sediment temperature was not a significant controlling factor of CH_4 flux at a sub-daily time scale, because its diurnal variation was <1.0℃ throughout the observation period (Fig. S3). Diffusive flux in other seasons also showed a similar tendency. The relationship between diffusive flux and wind speed (Fig. 5) confirmed the wind speed dependency. This wind speed dependence was consistent with previous studies, including a floating chamber observations in Liu et al. (2017) and gas-transfer velocity studies (Guérin et al., 2007; Heiskanen et al., 2014). Subsurface turbulence is enhanced by increasing wind speed (e.g., Wanninkhof et al., 2009), which explains the dependence of diffusive flux on wind speed.

For a given wind speed, the diffusive flux was higher in summer (Fig. 5). This is due to the difference in mean dissolved CH_4 concentration in the surface water caused by the seasonal variation of CH_4 production; the dissolved CH_4 concentration in the surface water derived from observations at one-month intervals (Fig. 3d) was 0.72 μmol L^{-1} in winter (January 25, 2018) and 1.49 μmol L^{-1} in summer (July 25, 2018). It should be noted that these data are not necessarily typical for the month because the mixing caused by strong wind can lead to a high variation of dissolved CH_4 concentration, even during stable stratification in summer due to the transfer of dissolved CH_4 from the bottom layer in this shallow lake. Formation of surface ice also led to the accumulation of dissolved CH_4 during winter (Fig. 3d). These unobserved variations in surface dissolved CH_4 concentration may partly explain the variability shown in Fig. 5.

313 To examine the effect of variation in surface dissolved CH_4 concentration on diffusive
314 flux, we separated the winter data into periods before surface ice formation and after ice melt
315 (Fig. 6a). After ice melt on February 22, the increase in diffusive flux with increasing wind speed
316 was higher than before ice formation. This was probably due to the high concentration of
317 dissolved CH_4 in the surface water after ice melt. The concentration of dissolved CH_4 in the
318 surface water on February 21 (i.e., immediately before the ice melt was complete) was 3.58 ±
319 0.15 μmol L^{-1} (Fig. 3d), which was the highest value observed in the surface water during the
320 study period. When the lake was covered with surface ice (January 27–February 21, 2018),
321 diffusive flux was poorly explained by wind speed (R^2 = 0.03, Fig. S4). Higher flux was also
322 observed during this period, likely caused by emissions through melted areas of the surface ice.

323 To examine the relationship of diffusive flux with wind speed during summer, the data
324 were separated based on the mean wind speed of the preceding 24 hours (Fig. 6b). When the
325 mean wind speed was low during the preceding 24 hours, it was assumed that dissolved CH_4
326 accumulated in the bottom layer, a condition under which the potential for diffusion increases.
327 We found that diffusive flux was higher for a given current wind speed when wind was calmer
328 during the preceding 24 hours. This suggests that the transfer of accumulated dissolved CH_4
329 from the bottom layer is an important factor influencing diffusive flux.

330 In the transfer velocity model, diffusive flux is estimated from the difference in
331 concentration between the thin surface water layer and the bulk surface water below. CH_4
332 concentration in surface water generally changes at sub-daily time scales in shallow lakes;
333 however, data on continuously measured dissolved CH_4 concentrations are scarce due to
334 technical constraints (e.g., Erkkilä et al., 2018). Therefore, continuous measurement of dissolved
335 CH_4 concentration is needed to evaluate the impacts of ice sheets during winter and transport of
336 CH_4-enriched bottom-layer water during summer on diffusive CH_4 emission from shallow lakes.
337

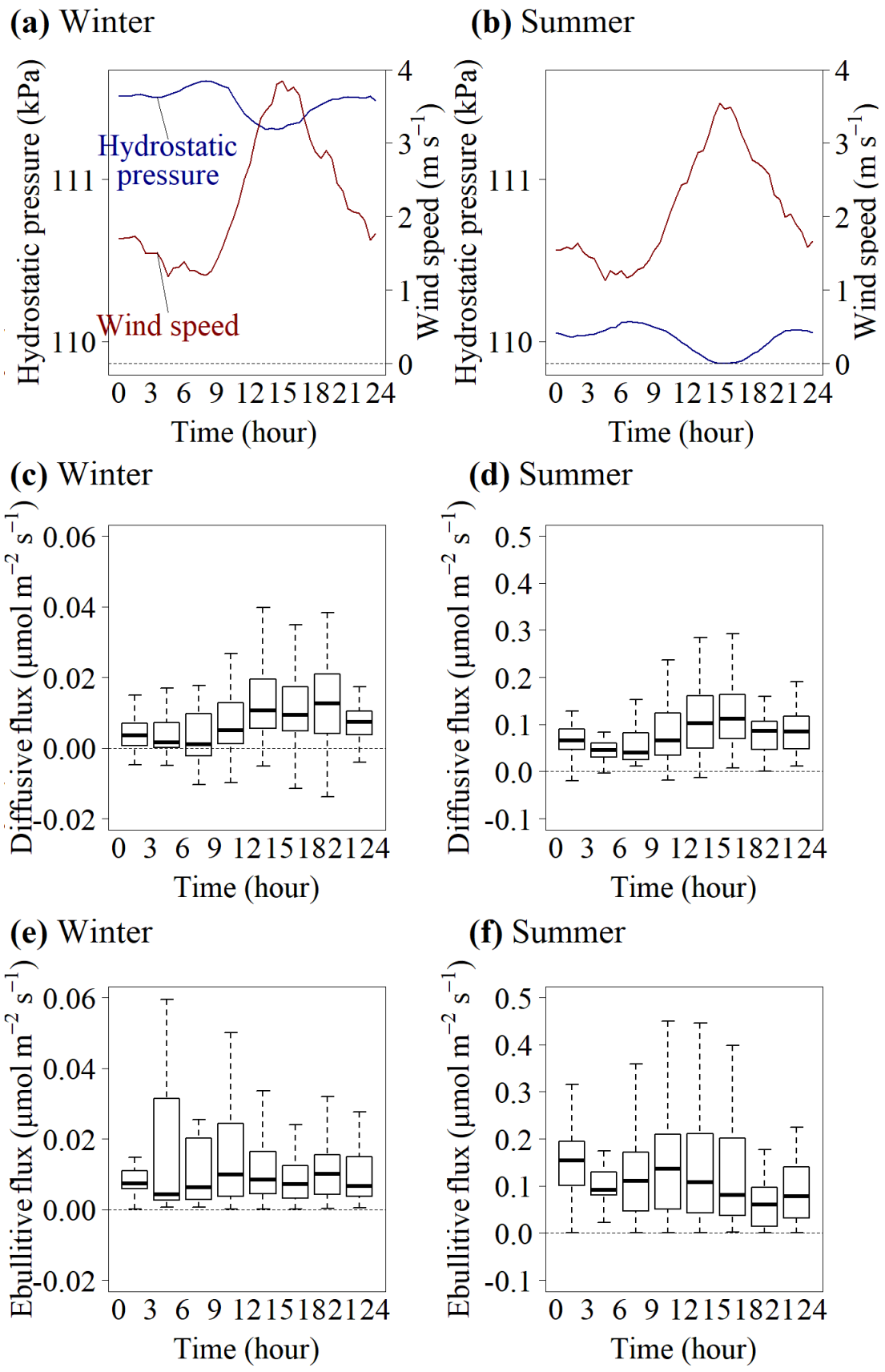
(a) Winter
(b) Summer
Hydrostatic pressure (kPa)
Wind speed (m s^{-1})
Hydrostatic pressure
Wind speed
Time (hour)
(c) Winter
(d) Summer
Diffusive flux (μmol m^{-2} s^{-1})
(e) Winter
(f) Summer
Ebullitive flux (μmol m^{-2} s^{-1})

338

Figure 4. Mean diurnal variation in **(a, b)** hydrostatic pressure (blue) and wind speed (red), **(c, d)** diffusive flux, and **(e, f)** ebullitive flux for winter (left panels) and summer (right panels). In the boxplots of **(c–f)**, the center lines represent median values, and the widths of the boxes show the interquartile ranges (IQR), and the whiskers represent maximum and minimum values within a range of median ± 1.5 × IQR. Data outside the range of the whiskers were not shown in these plots.

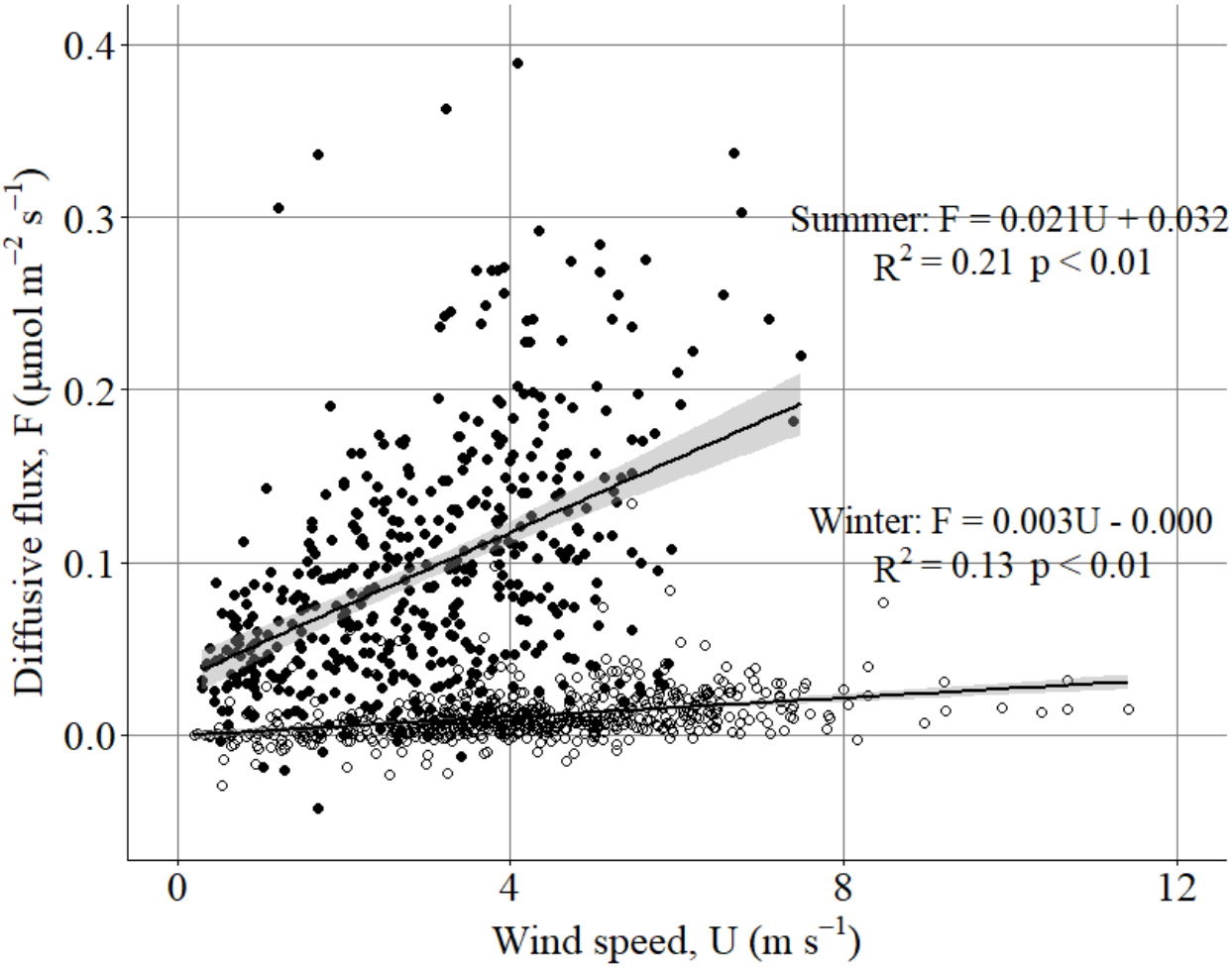

Figure 5. The relationship between wind speed and diffusive flux in winter (open circle) and summer (solid circle). Gray zones indicate 95% confidence intervals.

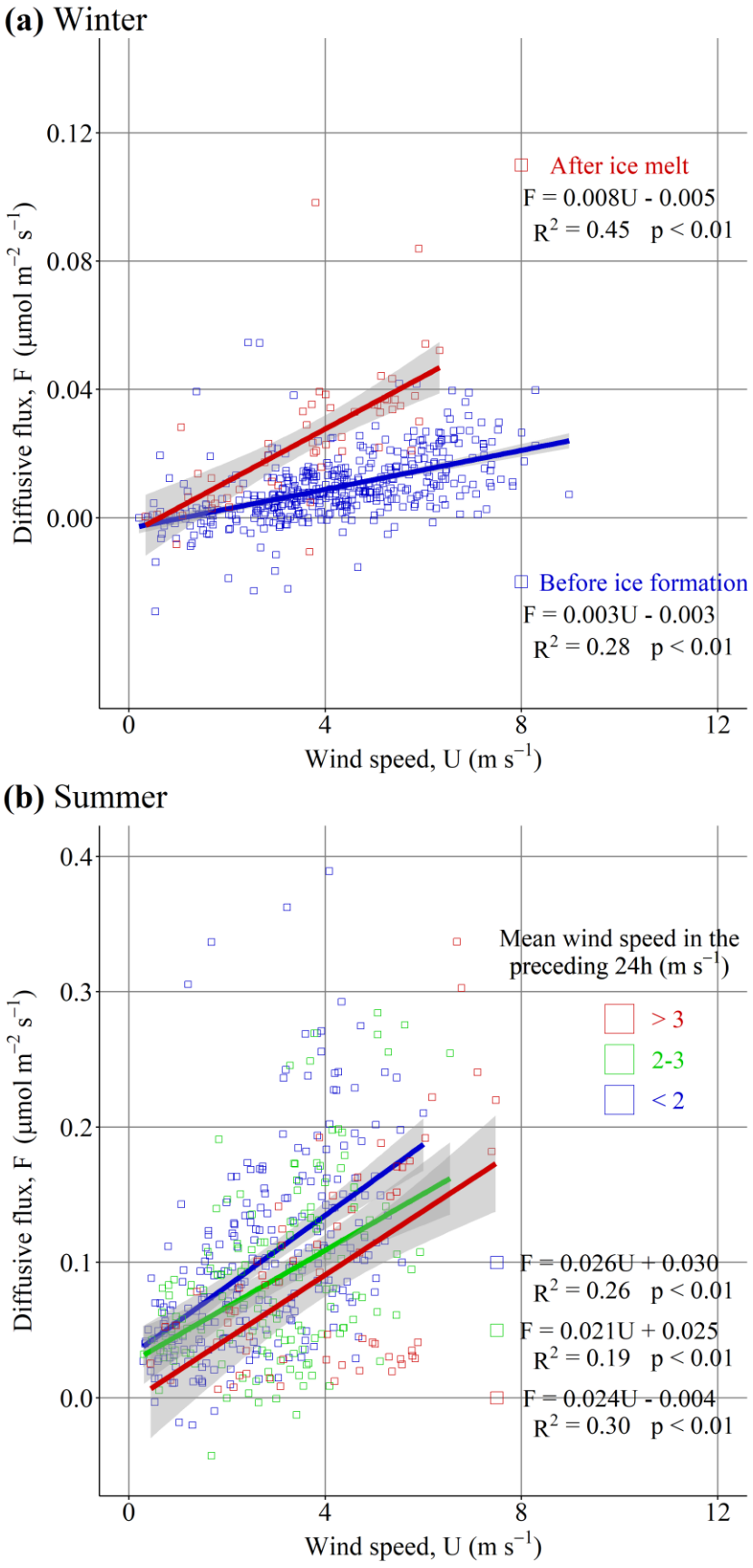
(a) Winter
After ice melt
F = 0.008U - 0.005
R2 = 0.45 p < 0.01
Before ice formation
F = 0.003U - 0.003
R2 = 0.28 p < 0.01
Diffusive flux, F (µmol m−2 s−1)
Wind speed, U (m s−1)
(b) Summer
Mean wind speed in the preceding 24h (m s−1)
> 3
2-3
< 2
F = 0.026U + 0.030
R2 = 0.26 p < 0.01
F = 0.021U + 0.025
R2 = 0.19 p < 0.01
F = 0.024U - 0.004
R2 = 0.30 p < 0.01
Diffusive flux, F (µmol m−2 s−1)
Wind speed, U (m s−1)

350

Figure 6. The relationship between wind speed and diffusive flux in (a) winter and (b) summer. (a) In winter, the data were separated into periods before surface ice formation (December 1 to January 26, blue points) and after ice melt (February 22 to 28, red points). (b) In summer, data were separated according to mean wind speed in the preceding 24 hours: blue points for <2 m s^{-1}, green points for 2–3 m s^{-1}, and red points for >3 m s^{-1}. Gray zones indicate 95% confidence intervals.

3.4 Short-term variation in ebullitive flux

In winter, higher ebullition was more frequently observed in the morning (3:00–12:00) (the upper quartile and whisker in Fig. 4e), with few high-flux observations in the afternoon (12:00–18:00). Ebullitive flux increased when wind speed began to increase (Fig. 4a), implying that wind was as a trigger for ebullition. However, ebullitive flux was not always high in the morning, as the median value was comparable to those for other time periods. In summer, no clear diurnal variation was observed for peak ebullitive flux (Fig. 4f), although the median values during 0:00–3:00 and 9:00–12:00 were slightly higher, and those during 3:00–6:00 and 18:00–21:00 slightly lower, than in other time periods. These slightly higher and lower ebullitive fluxes occurred during times of decreasing and increasing hydrostatic pressure, respectively, caused by atmospheric tides (Fig. 4b).

The responses of ebullitive flux to 30-min changes in wind speed and hydrostatic pressure were examined to elucidate environmental controls on ebullitive flux in detail (Fig. 7). When calculating the change in wind speed, wind speed data were smoothed using 5.5-h moving average before subtraction. In summer, the median and upper quartile of ebullitive flux were higher when hydrostatic pressure decreased ($\Delta P/\Delta t < 0$ in Fig. 7b). Increases in wind speed ($\Delta U/\Delta t > 0$) in combination with the decrease in pressure ($\Delta P/\Delta t < 0$) further enhanced ebullitive flux. These results are consistent with previous studies in which decreasing hydrostatic pressure (e.g., Tokida et al., 2007; Wik et al., 2013) and bottom shear stress caused by wind (e.g., Joyce and Jewell, 2003) were reported as triggers for ebullition. However, this pattern was not clear in winter (Fig. 7a).

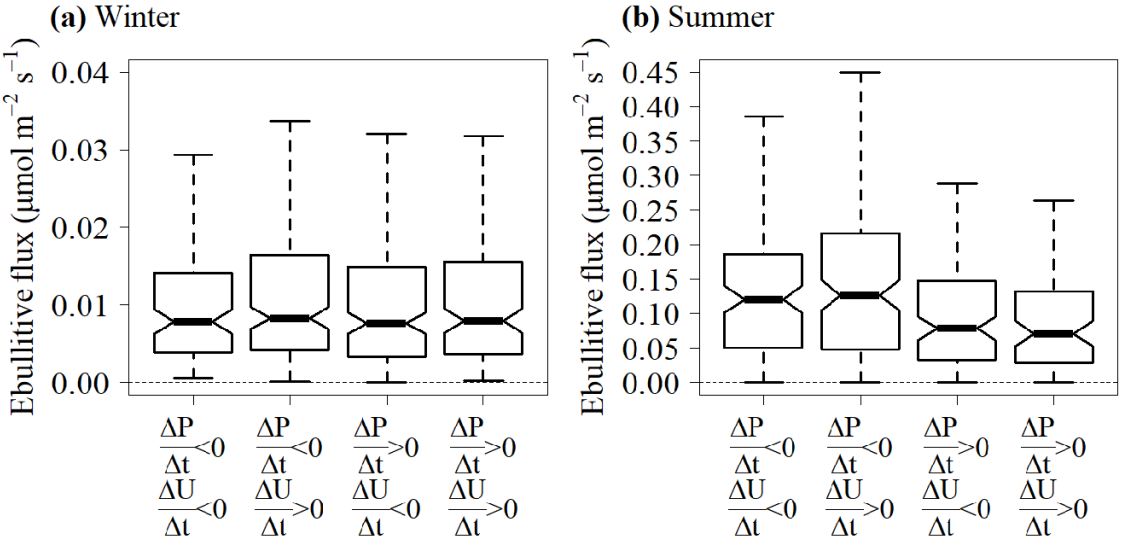

Figure 7. The effect of triggers (changes in hydrostatic pressure and wind speed) on ebullitive CH_4 flux in **(a)** winter and **(b)** summer. The data were divided into groups with different conditions: (1) decreasing pressure and wind speed; (2) decreasing pressure and increasing wind speed; (3) increasing pressure and decreasing wind speed; and (4) increasing pressure and wind speed. The boxplots are explained in the caption of **Fig. 4**. The notches represent 95% confidence intervals of medians.

The dependence of ebullitive flux on the magnitude of wind speed, rather than the change, was also investigated (Fig. S5). Ebullitive flux decreased with increasing wind speed in winter, although such a trend was not clear in summer.

In addition to the direct effect of triggers on ebullitive flux, the accumulation of bubbles in the sediment may be an important factor regulating the response of ebullitive flux to triggers. Under strong winds during winter, a decline in ebullitive flux was observed in the afternoon despite a continuous high wind speed (Fig. 8). Bubbles remaining in the sediment decrease as ebullition proceeds, and low temperatures slow the replenishment of bubbles, thus limiting ebullition. In summer, such a continuous decline in ebullitive flux was not observed.

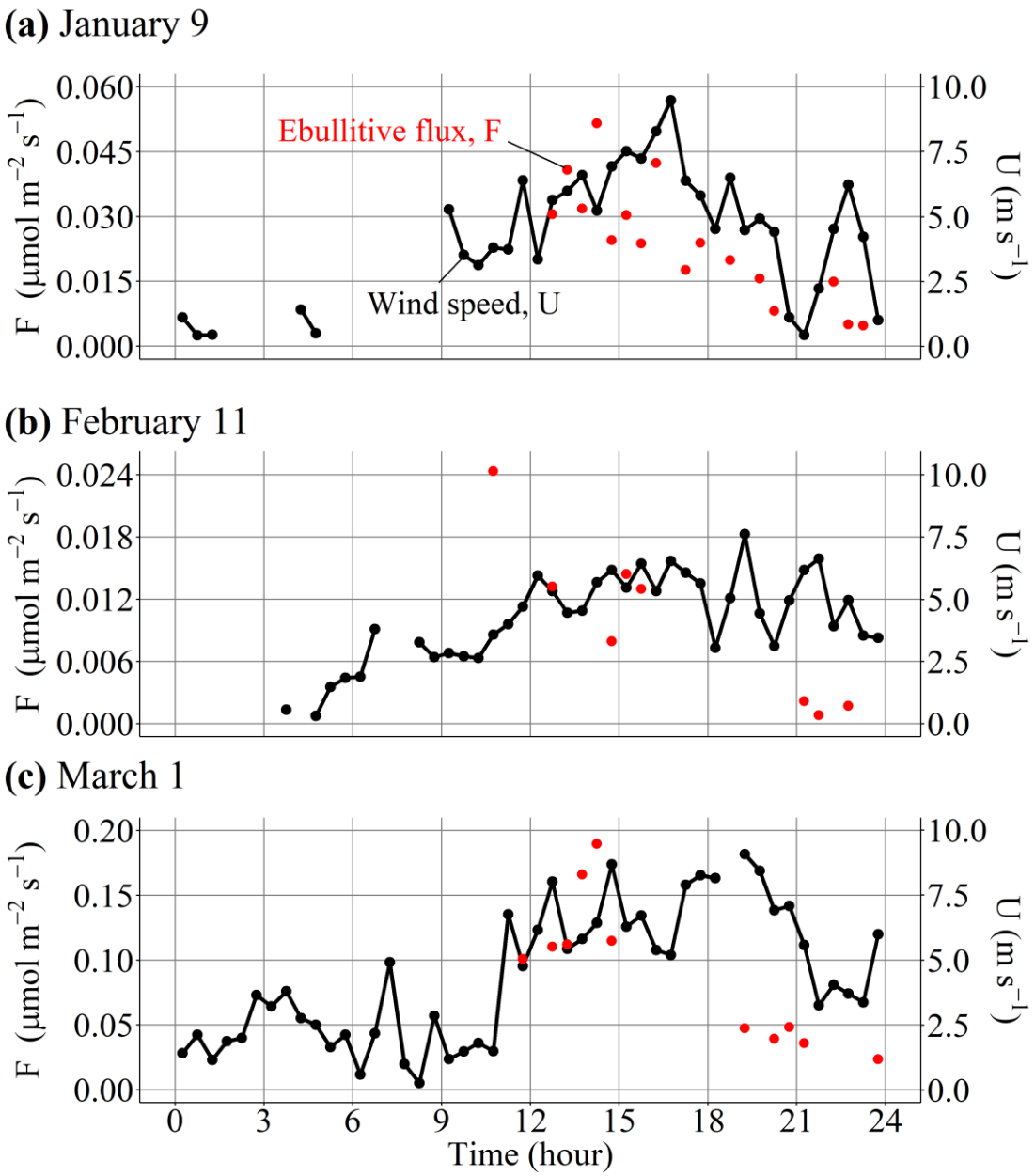

Figure 8. Case studies showing the variation in ebullitive CH_4 flux (red points) with wind speed (black line) in winter. The data are for **(a)** January 9, **(b)** February 11, and **(c)** March 1.

To further investigate how limited accumulation of sediment bubbles can affect ebullition, the relationships between median ebullitive flux at night (18:00–6:00) and the following morning (6:00–12:00) during cold (November–April, Fig. 9a) and warm months (May–October, Fig. 9b) were examined. In cold months, when high ebullitive flux (>0.05 μmol m^{-2} s^{-1}) was observed at night, the median ebullitive flux the following morning was generally lower. By contrast, when high ebullitive flux was not observed at night, high ebullitive flux tended to be observed the following morning. These relationships confirmed that winter

ebullitive flux is limited by the amount of bubble accumulation in the sediment, in addition to triggers such as changes in hydrostatic pressure and wind speed. Conversely, such relationships were not observed in summer, indicating that summer ebullitive flux is less limited by the amount of bubbles in the sediment because high rates of CH_4 production driven by high temperatures continuously replenish bubbles in the sediment. We also examined the relationship between ebullition in the morning and ebullition the following afternoon and found similar results (Fig. S6), indicating limited bubble accumulation in winter.

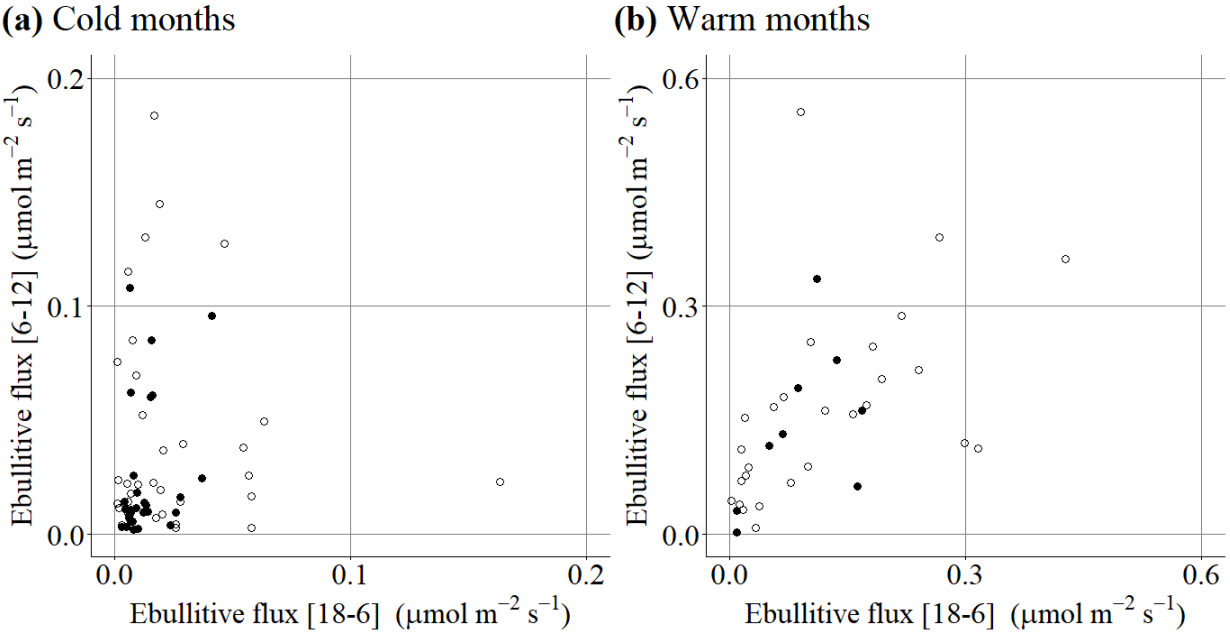

Figure 9. Scatter plots of the daily median ebullitive CH_4 flux at night (18:00–6:00) and the following morning (6:00–12:00) during (a) cold months (November–December in 2017 and January–April in 2018) and (b) warm months (September–October in 2017 and May–August in 2018). Black solid circles represent the median ebullitive flux with $n \geq 3$ for both the horizontal and vertical axes, while open circles represent those with $n < 3$.

The limited bubble accumulation in the sediments during winter provides insights into the different observed behaviors of ebullitive flux in winter and summer (Figs. 4 and 7). In winter, bubbles can accumulate in the sediment overnight when the wind speed is generally low (Fig. 4a) and are emitted to the atmosphere when wind speed begins to increase in the morning. In the afternoon, most of the accumulated bubbles have already been emitted to the atmosphere, so fewer remain in the sediment due to the lower CH_4 production rate in winter. This can lead to relatively clear diurnal patterns in ebullitive flux in winter (Fig. 4e). In winter, the amount of bubbles in the sediment is limited due to the low CH_4 production rate, and ebullition does not always occur even with triggers such as a decrease in hydrostatic pressure or increase in wind speed (Fig. 7a). In summer, the amount of accumulated bubbles was high enough due to the high CH_4 production rate that ebullition could occur any time there was a trigger (Fig. 7b). This led to relatively obscure diurnal patterns of ebullitive flux in summer (Fig. 4f). These results suggest

the importance of considering bubble accumulation in the sediments to explain variation in ebullitive flux at sub-daily time scales.

Podgrajsek et al. (2014) measured CH_4 flux using the eddy covariance technique in a boreal lake and showed that CH_4 flux tended to be high in the morning during spring and fall. The mean diurnal variation was similar to the variation in ebullitive flux observed at our site in winter. Although the authors suggested that disturbance of the water–sediment interface through convective turbulence could explain the high flux at night and early morning (Podgrajsek et al., 2014), our study also highlights the necessity of considering bubbles accumulated in the sediments. The similarity in diurnal variation of CH_4 flux suggests that ebullition in mid-latitude lakes may be limited by a lack of bubble accumulation in the sediment during cold months.

4 Conclusions

We measured CH_4 flux with the eddy covariance technique in a shallow eutrophic lake located in central Japan. We partitioned the total flux into diffusive and ebullitive fluxes, which enabled us to examine their environmental controls separately and in detail.

Mean total CH_4 flux was 0.03 μmol m^{-2} s^{-1} in winter and 0.21 μmol m^{-2} s^{-1} in summer. CH_4 flux was clearly higher in summer than winter; however, winter flux should not be ignored for accurate estimation of annual CH_4 flux. Diffusive and ebullitive flux contributed 44% and 56%, respectively, of total CH_4 flux, on average. Thus, both diffusion and ebullition are dominant pathways of CH_4 emitted to the atmosphere in this lake. Rough estimates of the annual mean diffusive and ebullitive fluxes were 17.6 and 19.3 g CH_4 m^{-2} $year^{-1}$, respectively, and total flux was 36.9 g CH_4 m^{-2} $year^{-1}$.

Diffusive flux increased as wind speed increased due to enhanced subsurface turbulence. Diffusive flux was higher in summer than in winter due to higher dissolved CH_4 concentration in the surface water. These results are consistent with those obtained using other methods such as floating chambers. Additionally, the transfer of accumulated dissolved CH_4 from the bottom layer to the surface in summer and accumulation of dissolved CH_4 under surface ice are important processes that explain the variability of diffusive flux.

Ebullition occurred following triggers such as a decrease in hydrostatic pressure or an increase in wind speed, consistent with previous studies. Using high time-resolution flux data, we further clarified the importance of considering bubbles accumulated in the sediments to explain the variation in ebullitive flux at sub-daily time scales. In winter, low CH_4 production slowed the replenishment of bubbles in the sediment, limiting ebullitive flux even when triggers occurred.

This study highlighted the power of the eddy covariance technique combined with flux partitioning as a general tool for elucidating the environmental controls underlying CH_4 flux in lakes, which are expected to depend on the lake properties. This will further improve our ability to predict CH_4 emission from lakes under climate change.

Acknowledgments

We would like to thank Mr. Hiroshi Moriyama for allowing us to use the pier for observations. This study was funded by a grant from the Japan Society for the Promotion of Science (JSPS) KAKENHI (no. 17H05039). Data sets used in this research are available online (http://science.shinshu-u.ac.jp/~hiwata/program.html).

References

Bastviken, D., Cole, J., Pace, M., and Tranvik, L. (2004), Methane emissions from lakes: dependence of lake characteristics, two regional assessments, and a global estimate. *Global Biogeochemical Cycle*, 18(4), GB4009. doi:10.1029/2004GB002238

Bastviken, D, Tranvik, L. J., Downing, J. A., Crill, P. M., Enrich-Prast A. (2011), Freshwater methane emissions offset the continental carbon sink. *Science*, 331, 50. doi:10.1126/science.1196808

Bock E. J., Hara, T., Frew, N. M., McGillis, W. R. (1999), Relationship between air-sea gas transfer and short wind waves. *Journal of Geophysical Research*, 104(C11), 821-831. doi:10.1029/1999JC900200

Cole, J. J. and Caraco, N. F. (1998), Atmospheric exchange of carbon dioxide in a low-wind oligotrophic lake measured by the addition of SF_6. *Limnology and Oceanography*, 43(4), 647-656. doi:10.4319/lo.1998.43.4.0647

De Bruin H. A. R., Kohsiek, W., and Van den Hurk B. J. J. M. (1993), A verification of some methods to determine the fluxes of momentum, sensible heat, and water vapor using standard deviation and structure parameter of scalar meteorological quantities. *Boundary-Layer Meteorology*, 63(3), 231-257. doi:10.1007/BF00710461

DelSontro, T., Boutet, L., St-Pierre, A., Giorgio, P. A., Prairie, Y. T. (2016), Methane ebullition and diffusion from northern ponds and lakes regulated by the interaction between temperature and system productivity. *Limnology and Oceanography*, 61(S1), S62-S77. doi:10.1002/lno.10335

Deshmukh, C., Serca, D., Delon, C., Tardif, R., Demarty, M., Jarnot, C., Meyerfeld, Y., Chanudet, V., Guédant, P., Rode, W., Descloux, S., and Guérin, F. (2014), Physical controls on CH_4 emissions from a newly flooded subtropical freshwater hydroelectric reservoir: Nam Theun 2. *Biogeosciences*, 11(15), 4251-4269. doi:10.5194/bg-11-4251-2014

Detto, M. and Katul, G. C. (2007), Simplified expressions for adjusting higher-order turbulent statistics obtained from open path gas analyzers. *Boundary-Layer Meteorology*, 122(1), 205-216. doi:10.1007/s10546-006-9105-1

Detto M., Verfaillie, J., Anderson, F., Xu, L., Baldocchi, D. (2011), Comparing laser-based open- and closed-path gas analyzers to measure methane fluxes using the eddy covariance

method. *Agricultural and Forest Meteorology*, 151(10), 1312-1324. doi:10.1016/j.agrformet.2011.05.014

Duc, N. T., Crill, P., and Bastviken, D. (2010), Implications of temperature and sediment characteristics on methane formation and oxidation in lake sediments. *Biogeochemistry*, 100(1-3), 185-196. doi:10.1007/s10533-010-9415-8

Erkkilä, K. M., Ojala, A., Bastviken, D., Biermann, T., Heiskanen, J. J., Lindroth, A., Peltola, O., Rantakari, M., Vesala, T., and Mammarella, I. (2018), Methane and carbon dioxide fluxes over a lake: comparison between eddy covariance, floating chambers, and boundary layer method. *Biogeosciences*, 15(2), 429-445. doi:10.5194/bg-15-429-2018

Eugster, W., DelSontro, T., and Sobek, S. (2011), Eddy covariance flux measurements confirm extreme CH_4 emissions from a Swiss hydropower reservoir and resolve their short-term variability. *Biogeosciences*, 8(9), 2815-1831. doi:10.5194/bg-8-2815-2011

Fechner-Levy, E. J. and Hemond, H. F. (1996), Trapped methane volume and potential effects on methane ebullition in a northern peatland. *Limnology and Oceanography*, 41(7), 1375-1383. doi:10.4319/lo.1996.41.7.1375

Forster, P., Ramaswamy, V., Artaxo, P., Berntsen, T., Betts, R., Fahey, D. W., Haywood, J., Lean, J., Lowe, D. C., Myhre, G., Nganga, J., Prinn, R., Raga, G., Schulz, M., and Van Dorland, R. (2007), Changes in Atmospheric Constituents and in Radiative Forcing. In: Climate Change 2007: The Physical Science Basis. Contribution of Working Group I to the Fourth Assessment Report of the Intergovernmental Panel on Climate Change. Cambridge University Press, Cambridge, United Kingdom and New York, NY, USA, 129-234.

Guérin, F., Abril, G., Serça, D., Delon, C., Richard, S., Delmas, R., Tremblay, A., and Varfalvy, L. (2007), Gas transfer velocities of CO_2 and CH_4 in a tropical reservoir and its river downstream. *Journal of Marine Systems*, 66(1-4), 161-172. doi:10.1016/j.jmarsys.2006.03.019

Heiskanen, J. J., Mammarell, I., Haapanala, S., Pumpanen, J., Vesala, T., Macintyre, S., and Ojala, A. (2014), Effects of cooling and internal wave motions on gas transfer coefficients in a boreal lake. *Tellus B*, 66(1), 22827. doi:10.3402/tellusb.v66.22827

Ikenaka, Y., Eun, H., Watanabe, E., Miyabara, Y. (2005), Sources, distribution, and inflow pattern of dioxins in the bottom sediment of Lake Suwa, Japan. *Bulletin of Environmental Contamination and Toxicology*, 75(5), 915-921. doi:10.1007/s00128-005-0837-2

Itoh, M., Kobayashi, Y., Chen, T. Y., Tokida, T., Fukui, M., Kojima, H., Miki, T., Tayasu, I., Shiah, F. K., and Okuda, N. (2015), Effect of interannual variation in winter vertical mixing on CH4 dynamics in a subtropical reservoir. *Journal of Geophysical Research: Biogeosciences*, 120(7), 1246-1261. doi:10.1002/2015JG002972

Itoh, M., Kojima, H., Ho, P.-C., Chang, C.-W., Chen, T.-Y., Hsiao, S. S.-Y., Kobayashi, Y., Fujibayashi, M., Kao, S.-J., Hsieh, C., Fukui, M., Okuda, N., Miki, T., and Shiah, F.-K. (2017),

Integrating isotopic, microbial, and modeling approaches to understand methane dynamics in a frequently disturbed deep reservoir in Taiwan. *Ecological Research*, 32(6), 861-871, doi:10.1007/s11284-017-1502-z

Iwata, H., Kosugi, Y., Ono, K., Mano, M., Sakabe, A., Miyata, A., Takahashi, K. (2014), Cross-validation of open-path and closed path eddy-covariance techniques for observing methane fluxes. *Boundary-Layer Meteorology*, 151(1), 95-118. doi:10.1007/s10546-013-9890-2

Iwata, H., Hirata, R., Takahashi, Y., Miyabara, Y., Itoh, M., and Iizuka, K. (2018), Partitioning eddy-covariance methane fluxes from a shallow lake into diffusive and ebullitive fluxes. *Boundary-Layer Meteorology*, 169(3), 413-428. doi:10.1007/s10546-018-0383-1

Jammet, M., Crill, P., Dengel, S., and Friborg, T. (2015), Large methane emissions from a subarctic lake during spring thaw: mechanisms and landscape significance. *Journal of Geophysical Research: Biogeosciences*, 120(11), 2289-2305. doi:10.1002/2015JG003137

Jammet, M., Dengel, S., Kettner, E., Parmentier, F. W., Wik, M., Crill, P., and Friborg, T. (2017), Year-round CH_4 and CO_2 flux dynamics in two contrasting freshwater ecosystems of the subarctic. *Biogeosciences*, 14(22), 5189-5216. doi:10.5194/bg-14-5189-2017

Jansen, J., Thornton, B. F., Jammet, M. M., Wik, M., Cortés, A., Friborg, T., MacIntyre, S., and Crill, P. M. (2019), Climate-sensitive controls on large spring emissions of CH_4 and CO_2 from northern lakes. *Journal of Geophysical Research: Biogeosciences*, 124(7), 2379-2399. doi:10.1029/2019JG005094

Joyce, J. and Jewell, P. W. (2003), Physical controls on methane ebullition from reservoirs and lake. *Environmental and Engineering Geosciences*, 9(2), 167-178. doi:10.2113/9.2.167

Kormann, R. and Meixner F. X. (2001), An analytical footprint model for non-neutral stratification. *Boundary-Layer Meteorology*, 99(2), 207-224. doi:10.1023/A:1018991015119

Liikanen, A., Huttunen, J. T., Murtoniemi, T., Tanskanen, H., Väisänen, T., Silvola, J., Alm, J., and Martikainen, P. J. (2003), Spatial and seasonal variation in greenhouse gas and nutrient dynamics and their interactions in the sediments of a boreal eutrophic lake. *Biogeochemistry*, 65(1), 83-103. doi:10.1023/A:1026070209387

Liu, L., Xu, M., Li, R., and Shao, R. (2017), Timescale dependence of environmental controls on methane efflux from Poyang Hu, China. Biogeosciences, 14(8), 2019-2032. doi:10.5194/bg-14-2019-2017

MacIntyre, S., Jonsson, A., Jansson, M., Aberg, J., Turney, D. E. and Miller, S. (2010), Buoyancy flux, turbulence, and the gas transfer coefficient in a stratified lake. *Geophysical Research Letters*, 37(24), L24604. doi:10.1029/2010GL044164

610 Magen, C., Lapham, L. L., Pohlman, J. W., Marshall, K., Bosman, S., Casso, M., Chanton, J. P.
611 (2014), A simple headspace equilibration method for measuring dissolved methane. *Limnology*
612 *and Oceanography: Methods*, 12(9), 637-650. doi:10.4319/lom.2014.12.637
613
614 Mahrt, L. (1998), Flux sampling errors for aircraft and towers. *Journal of Atmospheric and*
615 *Oceanic Technology*, 15(2), 416-429. doi:10.1175/1520-
616 0426(1998)015<0416:FSEFAA>2.0.CO;2
617
618 McDermitt, D., Burba, G., Xu, L., Anderson, T., Komissarov, A., Riensche, B., Schedlbauer, J,
619 Starr, G., Zona, D., Oechel, W., Oberbauer, S., and Hastings, S. (2011), A new low-power, open-
620 path instrument for measuring methane flux by eddy covariance. *Applied Physics B*, 102(2), 391-
621 405. doi:10.1007/s00340-010-4307-0
622
623 Park, H., Iwami, C., Watanabe, M. F., Harada, K., Okino, T., Hayashi, H. (1998), Temporal
624 variabilities of the concentrations of intra- and extracellular microcystin and toxic microcystis
625 species in a hypertrophic lake, Lake Suwa, Japan (1991-1994). *Environmantal Toxicology and*
626 *Water Quality*, 13(1), 61-72. doi:10.1002/(SICI)1098-2256(1998)13:1<61::AID-
627 TOX4>3.0.CO;2-5
628
629 Podgrajsek, E., Sahlée, E., and Rutgersson, A. (2014), Diurnal cycle of lake methane flux.
630 *Journal of Geophysical Research: Biogeosciences*, 119(3), 236-248. doi:10.1002/2013JG002327
631
632 Podgrajsek, E., Sahlée, E., Bastviken, D., Natchimuthu, S., Kljun, N., Chmiel, H. E.,
633 Klemedtsson, L., and Rutgersson, A. (2016), Methane fluxes from a small boreal lake measured
634 with the eddy covariance method. *Limnology and Oceanography*, 61(S1), S41-S50.
635 doi:10.1002/lno.10245
636
637 Rey-Sanchez, A. C., Morin, T. H., Stefanik, K. C., Wrighton, K., and Bohrer, G. (2018),
638 Determining total emissions and environmental drivers of methane flux in a Lake Erie estuarine
639 marsh. *Ecological Engineering*, 114(15), 7-15. doi:10.1016/j.ecoleng.2017.06.042
640
641 Saunois, M., Bousquet, P., Poulter, B., Peregon, A., Ciais, P., Canadell, J. G., Dlugokencky, E.
642 J., Etiope, G., Bastviken, D., Houweling, S., Janssens-Maenhout, G., Tubiello, F. N., Castaldi, S.,
643 Jackson, R. B., Alexe, M., Arora, V. K., Beerling, D. J., Bergamaschi, P., Blake, D. R.,
644 Brailsford, G., Brovkin, V., Bruhwiler, L., Crevoisier, C., Crill, P., Covey, K., Curry, C.,
645 Frankenberg, C., Gedney, N., Höglund-Isaksson, L., Ishizawa, M., Ito, A., Joos, F., Kim, H.-S.,
646 Kleinen, T., Krummel, P., Lamarque, J.-F., Langenfelds, R., Locatelli, R., Machida, T.,
647 Maksyutov, S., McDonald, K. C., Marshall, J., Melton, J. R., Morino, I., Naik, V., O'Doherty, S.,
648 Parmentier, F.-J. W., Patra, P. K., Peng, C., Peng, S., Peters, G. P., Pison, I., Prigent, C., Prinn,
649 R., Ramonet, M., Riley, W. J., Saito, M., Santini, M., Schroeder, R., Simpson, I. J., Spahni, R.,
650 Steele, P., Takizawa, A., Thornton, B. F., Tian, H., Tohjima, Y., Viovy, N., Voulgarakis, A., van
651 Weele, M., van der Werf, G. R., Weiss, R., Wiedinmyer, C., Wilton, D. J., Wiltshire, A.,
652 Worthy, D., Wunch, D., Xu, X., Yoshida, Y., Zhang, B. Zhang, Z., and Zhu, Q. (2016), The
653 global methane budget 2000-2012. *Earth System Science Data*, 8(2), 697-751. doi:10.5194/essd-
654 8-697-2016
655

Schotanus P., Nieuwstadt F. T. M, and de Bruin H. A. R. (1983), Temperature measurement with a sonic anemometer and its application to heat and moisture fluxes. *Boundary-Layer Meteorology*, 26(1), 81–93. doi:10.1007/BF00164332

Schubert, C. J., Diem, T., and Eugster, W. (2012), Methane emissions from a small wind shielded lake determined by eddy covariance, flux chambers, anchored funnels, and boundary model calculations: a comparison. *Environmental Science and Technology*, 46(8), 4515-4522. doi:10.1021/es203465x

Stepanenko, V., Mammarella, I., Ojala, A., Miettinen, H., Lykosov, V., and Veesala, T. (2016), LAKE 2.0: a model for temperature, methane, carbon dioxide and oxygen dynamics in lakes. *Geoscientific Model Development*, 9(5), 1977-2006. doi:10.5194/gmd-9-1977-2016

Subin, Z. M., Murphy, L. N., Li, F., Bonfils, C., and Riley, W. J. (2012), Boreal lakes moderate seasonal and diurnal temperature variation and perturb atmospheric circulation: analysis in the Community Earth System Model 1 (CESM1). *Tellus A*, 64(1), 15639. doi:10.3402/tellusa.v64i0.15639

Tedford, E. W., MacIntyre, S., Miller, S. D., and Czikowsky, M. J. (2014), Similarity scaling of turbulence in a temperate lake during fall cooling. *Journal of Geophysical Research: Oceans*, 119(8), 4689-4713. doi:10.1002/2014JC010135

Thebrath, B., Rothfuss, F., Whiticar, M. J., and Conrad, R. (1993), Methane production in littoral sediment of Lake Constance. *FEMS Microbiology Ecology*, 11(3-4), 279-289. doi:10.1111/j.1574-6968.1993.tb05819.x

Tokida, T., Miyazaki, T., and Mizoguchi, M., Nagata, O., Takakai, F., Kagemoto, A., and Hatano, R., (2007), Falling atmospheric pressure as a trigger for methane ebullition from peatland. *Global Biogeochemical Cycles*, 21(2), GB2003. doi:10.1029/2006GB002790

Utsumi, M., Nojiri, Y., Nakamura, T., Nozawa, T., Otsuki, A., and Seki, H. (1998), Oxidation of dissolved methane in a eutrophic, shallow lake: Lake Kasumigaura, Japan. *Limnology and Oceanography*, 1998, 43(3), 471−480. doi:10.4319/lo.1998.43.3.0471

van de Boer, A., Moene, A. F., Graf, A., Schüttemeyer, D., and Simmer, C. (2014), Detection of entrainment influences on surface-layer measurements and extension of Monin-Obukov similarity theory. *Boundary-Layer Meteorology*, 152(1), 19-44. doi:10.1007/s10546-014-9920-8

Vickers, D. and Mahrt, L. (1997), Quality control and flux sampling problems for tower and aircraft data. *Journal of Atmospheric and Oceanic Technology*, 14(3), 512-526. doi:10.1175/1520-0426(1997)014<0512:QCAFSP>2.0.CO;2

Wanninkhof, R., Asher, W. E., Ho, D. T., Sweeney, C., and McGillis, W. R. (2009), Advanced in quantifying air-sea gas exchange and environmental forcing. *Annual Review of Marine Science*, 1, 213-244. doi:10.1146/annurev.marine.010908.163742

Webb, E. K., Pearman, G. L. and Leuning, R. (1980), Correction of flux measurements for density effects due to heat and water vapor transfer. *Quarterly Journal of the Royal Meteorological Society*, 106, 85-100. doi:10.1002/qj.49710644707

Wik, M., Patrick, M. C., Varner, R. K., and Bastviken, D. (2013), Multiyear measurements of ebullitive methane flux from three subarctic lakes. *Journal of Geophysical Research: Biogeosciences*, 118(3): 1307-1321. doi:10.1002/jgrg.20103